Experimental and Theoretical Study of Quasicoherent Fluctuations in Enhanced D_α Plasmas in the Alcator C-Mod Tokamak

A. Mazurenko, M. Porkolab, D. Mossessian, and J. A. Snipes
Plasma Science and Fusion Center, Massachusetts Institute of Technology, Cambridge, Massachusetts 02139

X. Q. Xu and W. M. Nevins
Lawrence Livermore National Laboratory, Livermore, California 94551

(Received 20 November 2001; revised manuscript received 2 August 2002; published 12 November 2002)

A comparison of experimental measurements and theoretical studies of the quasicoherent (QC) mode, observed at high densities during enhanced D_α (EDA) H mode in the Alcator C-Mod tokamak, are reported. The QC mode is a high frequency (~ 100 kHz) nearly sinusoidal fluctuation in density and magnetic field, localized in the steep density gradient ("pedestal") at the plasma edge, with typical wave numbers $k_R \approx 3$–$6\ \mathrm{cm}^{-1}$, $k_\theta \approx 1.3\ \mathrm{cm}^{-1}$ (midplane). It is proposed here that the QC mode is a form of resistive ballooning mode known as the resistive X-point mode, in reasonable agreement with predictions by the BOUT (boundary-plasma turbulence) code.

DOI: 10.1103/PhysRevLett.89.225004 PACS numbers: 52.35.Ra, 52.55.Fa, 52.65.Kj, 52.70.Kz

The high confinement (H mode) regime in magnetically confined high temperature plasmas in toroidal configurations is characterized by a significant increase in the energy confinement time (as compared to L mode, or low confinement) due to the formation of a transport barrier at the plasma edge [1] and is a highly desirable mode of operation in future fusion reactors. Depending on operating conditions, different types of H modes have been observed in past experiments. ELMy (edge localized mode, a macroscopic instability) H-mode plasmas are characterized by the periodic occurrence of a macroscopic instability near the plasma edge that cleanses impurities from the core plasma [2]. The ELM-free H mode is free of any large scale instability at the edge; however, owing to the excellent particle confinement, high-Z impurity accumulation in the plasma core eventually leads to a radiative collapse [3]. In the high density, compact, diverted Alcator C-Mod tokamak at MIT ($R = 0.67$ m, $a = 0.22$ m, $B_T \approx 5.3$ T, $I_P \geq 0.8$ MA, $\kappa \approx 1.7$, $q_{95} \geq 3.5$, $n_0 \approx 4 \times 10^{20}\ \mathrm{m}^{-3}$), yet another kind of H mode is observed, the enhanced D_α (EDA) H mode [3]. The plasma in this regime is characterized by significantly reduced impurity confinement compared to the ELM-free H mode, with only marginally lower energy confinement. The EDA H mode is an excellent candidate for long pulse or steady-state operation. The EDA H mode is accompanied by a continuous, high frequency (~ 100 kHz) "quasicoherent" (QC) fluctuation, localized in the steep density gradient (pedestal) at the plasma edge. The QC mode is believed to be responsible for the reduced particle (and impurity) confinement, yet allowing good energy confinement in the EDA H mode.

A similar mode was found earlier on the neutral beam heated poloidal divertor experiment (PDX) tokamak [4], although in the neutral beam heated PDX the fluctuations were always bursting in time, whereas in C-Mod the QC mode is typically continuous. In the Alcator C-Mod tokamak, the QC mode is observed by several diagnostics, including phase contrast imaging, a reflectometer, and scanning Langmuir and magnetic probes [5].

In this Letter, we present detailed measurements of the QC mode using the phase contrast imaging (PCI) diagnostic and comparisons with theoretical predictions. The PCI measures line integrated density fluctuations along 12 vertical chords (Fig. 1). This geometry makes the PCI sensitive to fluctuations that have a wave number k_R across the laser beam in the range $1.5\ \mathrm{cm}^{-1} < |k_R| < 10\ \mathrm{cm}^{-1}$ (limited by the beam 3.5 cm width on the low side and by the 0.3 cm chord spacing on the high side). The typical wave number of the QC mode is found to be $k_R \sim 3$–$6\ \mathrm{cm}^{-1}$. The PCI lacks vertical localization capabilities, being sensitive to Fourier components of the density fluctuations having $k_Z \approx 0$. However, reflectometer [6] and scanning probe measurements [7] show that the mode is localized in the pedestal region. The poloidal wave number of the mode, k_θ, may be related to k_R using the condition that $k_Z \approx 0$, so that $|k_\theta| \approx |k_R| \sin\zeta \sim 3$–$5\ \mathrm{cm}^{-1}$ where ζ is the angle between the separatrix and the vertical at the locations where the PCI chords cross the plasma edge.

The time evolution of the mode frequency spectrum is shown in Fig. 2. The QC mode typically appears with a frequency of 200–250 kHz following the transition from the "low confinement" (L mode) to the EDA H mode at 0.78 s. It then sweeps down in frequency to a steady-state value of 60–120 kHz. The spectrum is quite narrow at all times with $\Delta f/f \sim 0.05$–0.2 (full width at half maximum). The time scale for this frequency evolution is $\sim$50 ms, comparable to the momentum confinement time [8]. The mode wave number, as well as the major pedestal parameters, vary by less than 20% during this frequency sweep, suggesting that the frequency change is caused by changes in the plasma rotation (an interpretation supported by simulations reported below).

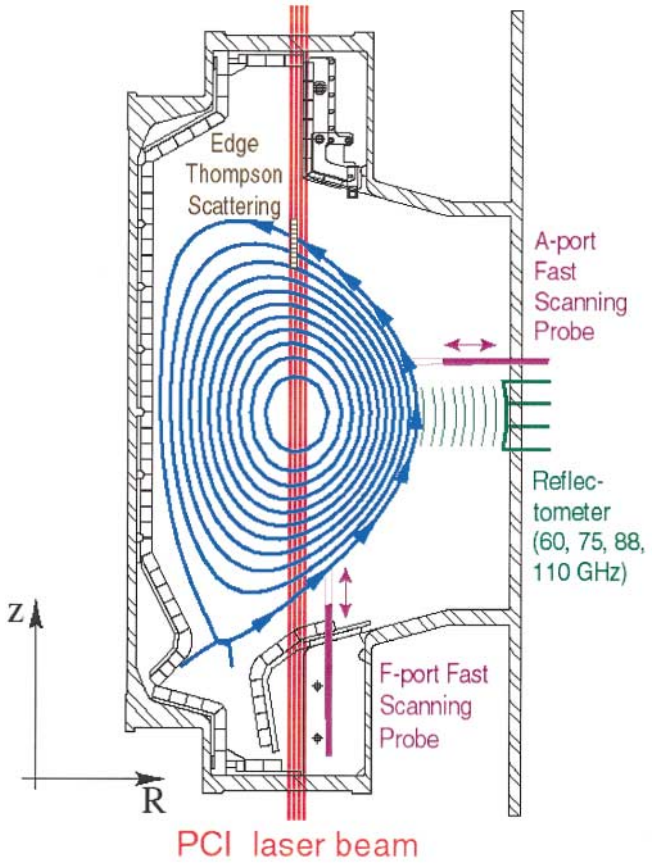

FIG. 1 (color). Experimental setup and plasma cross section of C-Mod. The laser beam of the PCI diagnostic passes vertically through the plasma to a phase plate and a detector array (not shown). The arrows depict the location and the direction of propagation of the QC mode.

Figure 3 illustrates the QC-mode frequency-wave number spectrum, as observed by the PCI. The mode shows up as the two strong peaks at $f = 95$ kHz and $k_R = -4$ and $+5$ cm^{-1}. Correlations between signals from two Langmuir probes momentarily inserted (a scanning probe) into the plasma edge [8] show that the mode propagates in the electron diamagnetic drift direction. The PCI laser detects poloidally propagating edge fluctuations both at the top (generating the PCI signal at negative k_R) and at the bottom (generating the PCI signal at positive k_R), resulting in two peaks in the PCI spectrum [9]. The small asymmetry of this spectrum with k_R results from up/down asymmetries of the C-Mod equilibrium, which result in differences in the angle between the separatrix and the PCI laser beam at the top ($\zeta_{\text{top}} = -62°$) and bottom ($\zeta_{\text{bottom}} = 51°$) separatrix crossings; as well as a nonzero ballooning-mode angle for the QC mode (e.g., the BOUT simulations described below find $k_r \approx -0.8$ cm^{-1} at the outboard midplane).

The typical QC-mode poloidal wave number inferred from the PCI diagnostic is $k_\theta \sim 4$ cm^{-1}, which corresponds to a relatively high poloidal mode number of $m \sim 100$. Higher harmonics of the mode typically are not detected, suggesting that the fluctuation is sinusoidal. This is in contrast to the edge harmonic oscillations observed in the DIII-D tokamak where many harmonics are typically seen [10].

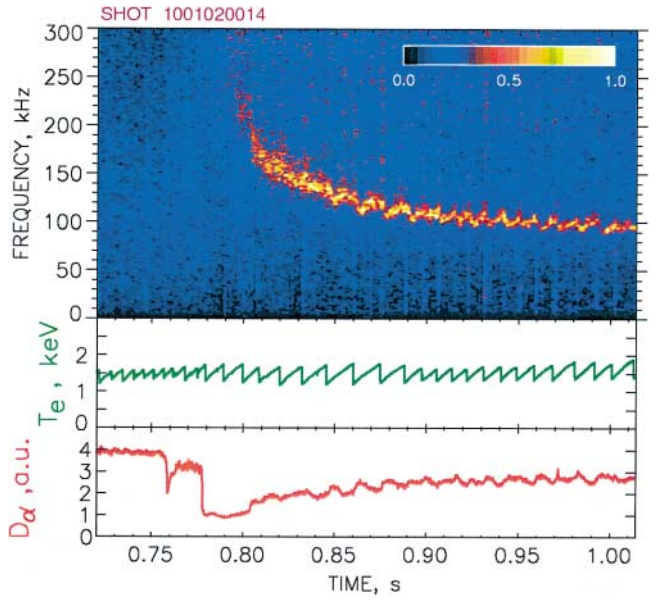

FIG. 2 (color). Time sequence showing the QC mode starting at about 0.79 sec following an L-H transition. Also shown are traces of central T_e and the D_α emission line intensity.

The magnetic component of the QC fluctuation has been measured with a coil in the tip of a scanning probe [11]. This coil was oriented to measure the poloidal component of δB. When positioned within $\sim$2 cm of the separatrix during an EDA H mode, the QC mode is detected with an amplitude (rms) of $\sim$1.5 G or about 0.004% of the total magnetic field. This magnetic

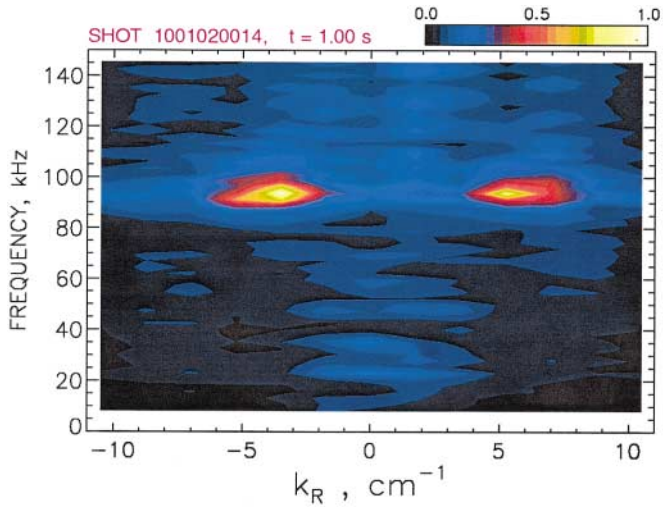

FIG. 3 (color). Two-dimensional spectrum of the 12 PCI signals. Positive k_R correspond to fluctuations propagating across the PCI beam in the direction of increase of major radius R, negative k_R in the direction of decrease of R. Two separate peaks for QC mode appear since the mode is detected twice—once on the top and once at the bottom of the plasma.

perturbation falls off rapidly with distance, as expected with a high wave-number mode.

It has been suggested that the QC mode is a resistive ballooning mode [12]. We believe that the QC mode may be a particular form of resistive ballooning mode known as the resistive X-point mode [13,14] and investigate this hypothesis through detailed comparison between experimental measurements and the recently developed boundary-plasma turbulence code (BOUT) [13]. BOUT models radially localized boundary-plasma turbulence in realistic divertor geometry using the Braginskii (collisional, two-fluid) equations for the evolution of plasma vorticity, density (n_i), electron and ion temperatures (T_e, T_i), and parallel momentum. Although BOUT contains many sources of free energy which can drive plasma turbulence, it has been found that the dominant instability in BOUT simulations of the C-Mod EDA H mode (and in some DIII-D simulations as well [13]) is the resistive X-point mode (a resistive ballooning mode which is strongly influenced by the magnetic geometry near the X point). The large pressure gradient in the pedestal region, together with locally unfavorable magnetic curvature drives this mode. It is radially localized to pedestal and is electromagnetic at the outboard midplane ($\partial\phi/ds \approx i\omega A_\parallel$), transitioning to an electrostatic resistive mode ($A_\parallel \approx 0$) near the X point. This transition, breaking the ideal MHD constraint that the magnetic field is frozen into the plasma, is allowed because nonideal terms related to electron dissipation and inertia (the collisional and collisionless skin effects) which are proportional to $k_\perp^2$ become large near the X point where magnetic shear yields large radial wave number k_r, while $B_\theta \rightarrow 0$ yields large k_θ [14].

We start our BOUT simulations using an EDA H-mode plasma profile corresponding to the time slice at 976 ms of the C-Mod discharge 1001020014 (i.e., the discharge shown in Figs. 2 and 3). The magnetic geometry is obtained from the magnetic equilibrium code EFIT [15], which is run on a 129×129 grid and includes the bootstrap current contribution. The equilibrium plasma profiles are obtained by using hyperbolic tangent fits to the experimentally determined plasma density n_e and electron temperature T_e. The midplane temperature and density on the separatrix are $T_e = 50$ eV and $n_e = 1.2 \times 10^{20}$ m^{-3}, respectively, while at the top of the pedestal, $T_e = 300$ eV and $n_e = 4 \times 10^{20}$ m^{-3}. For these parameters ν^* varies from five to several hundred over the boundary region (normalized poloidal flux, $\psi_n > 95\%$). The mean free path for electron-ion collisions is less than the connection length ($q_{95}R_0 \approx 230$ cm, where q_{95} is the safety factor at $\psi_n = 0.95$) over the entire simulation volume, varying from 230 cm at the boundary between the BOUT simulation volume and the plasma core (~ 1 cm inside the separatrix at the outboard midplane) to 3.5 cm in the far scrape-off layer (~ 1 cm outside the separatrix at the outboard midplane). This high collisionality justifies both the assumption $T_i \approx T_e$ (the edge T_i profile is not routinely measured in C-Mod) and the validity of the Braginskii fluid equations.

During the first 15 μs of the simulation, we observe linear growth of a classic resistive X-point mode [14] (that is, a linear instability localized along the magnetic field by dissipation at the X points with a radial extent less than the pedestal width) at a frequency $f \approx 400$ kHz, with growth rate $\gamma_{\rm lin} \approx 6 \times 10^5$ s^{-1} and midplane poloidal wave number $k_\theta \approx 5$ cm^{-1}. Over the following 20 μs, the instability saturates, there is an inverse cascade to $k_\theta \approx 1.3$ cm^{-1}, and the radial electric field evolves to a self-consistent, steady-state profile.

We observe a remarkably coherent resistive X-point mode over the final 100 μs of the simulation. This mode has a radial scale length for the scalar and vector potentials which is greater than the width of the pedestal. In this respect, it resembles the surface wave described by Rogers and Drake [16]. In particular, after the inverse cascade the poloidal wave number at the outboard midplane is in reasonable agreement with their estimate, $k_\theta \approx (\rho_s^2 R)^{-1/3} \approx 1.45$ cm^{-1}.

Figure 4 shows the radial profiles from the BOUT simulation of the equilibrium density, the density fluctuation (rms), the magnetic field fluctuation (rms), and the radial electric field at the outboard midplane. The density fluctuations and the E_r well are localized about the maximum density gradient in the edge pedestal, about 2 mm inside the separatrix in these simulations. The rms density fluctuation at the pedestal midpoint has a relative amplitude of 36% with a full width at half maximum of 5 mm, while the rms fluctuating potential is about 80 V at the same location, in reasonable agreement with measurements of $\delta n/n \approx 30\%$ and $\delta\phi_{\rm rms} \approx 85$ V on other C-Mod shots [11]. The peak amplitude of the fluctuating poloidal magnetic field seen in BOUT at the outboard midplane is 20 G. The magnetic perturbation falls off rapidly in the scrape-off layer, reaching a value of ~ 1 G at a distance of 1 cm from the separatrix. Similar values of δB_θ at this location have been observed on magnetic probes [11].

The BOUT simulations also support our interpretation that the downward sweep in the quasicoherent mode frequency observed in Fig. 2 results from changes in the edge plasma rotation. In a sequence of BOUT simulations, the frequency of the quasicoherent mode varied from 400 to 40 kHz (with only small changes in the k_θ spectrum) as the plasma rotation velocity at the boundary between the BOUT simulation volume and the core plasma was varied from -3 to $+9$ km/s (corresponding to radial electric fields from -13 to $+40$ kV/m). For a reasonable choice of 5.3 km/s (corresponding to a radial electric field of 22 kV/m), the modeling reproduces the observed QC mode frequency of $f \approx 100$ kHz at $k_\theta - 1.3$ cm^{-1} (propagation in the electron diamagnetic drift direction). Such large radial electric fields have been inferred near the C-Mod plasma edge in past experiments [17].

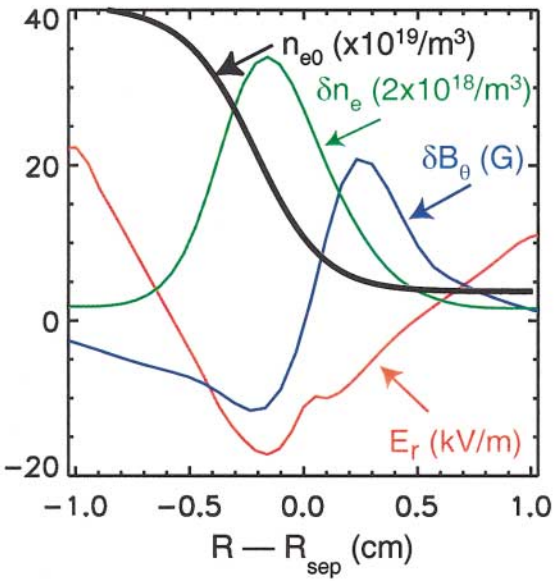

FIG. 4 (color). Radial profiles of background plasma density (chosen to match the C-Mod discharge shown in Figs. 2 and 3), density perturbation (rms), poloidal magnetic field perturbation (rms), and radial electric field at outboard midplane from BOUT simulations.

The poloidal wave number is in agreement with the published probe data [7,11], while the frequency and linewidth are essentially the same as those seen by the PCI (see Fig. 2). It follows [14] from the conservation of toroidal mode number and the relation $k_\phi = n/R$ that the poloidal wave number k_θ for ballooning modes (for which $\boldsymbol{k} \cdot \boldsymbol{B} \approx 0$, or $k_\theta B_\theta \approx -k_\phi B_\phi$) varies within a flux surface as $k_\theta(\theta_1)/k_\theta(\theta_2) \approx [B_\theta(\theta_2)R_2^2]/[B_\theta(\theta_1)R_1^2]$. This poloidal variation in k_θ is observed in both the C-Mod experiments (comparing midplane measurements of k_θ with that inferred from the PCI measurements) and the BOUT simulations. In these simulations $k_\theta = -2.6$ cm^{-1} at the top PCI scattering location and $k_\theta = -2.8$ cm^{-1} at the bottom PCI scattering location. Recalling that the PCI diagnostic is sensitive to the components of the density fluctuation with $k_Z \approx 0$, so that $|k_R| \approx |k_\theta|/\sin\zeta$, the corresponding values of k_R are -3.2 and $+3.6$ cm^{-1}, respectively, reproducing the small anisotropy observed in the PCI k_R spectrum and in reasonable agreement regarding the magnitude of k_R.

Initial results from BOUT simulations scans in both q_{95} and collisionality show that the quasicoherent mode disappears (leaving a quiescent edge plasma) as q_{95} is reduced from 3.0 to 2.5 at constant edge temperature and pressure, or as the temperature is increased (that is, the collisionality is reduced) at constant q_{95} and pressure. This is in qualitative agreement with C-Mod experiments, where the QC mode vanishes (yielding an ELM-free H mode) for $q_{95} \leq 3.5$, or at low density (i.e., low edge collisionality) [7].

In conclusion, we have presented the first experimental measurements of the frequency and wave number of the QC mode by a nonintrusive diagnostic (the PCI). Measurements of the QC mode using the PCI, and other diagnostics, are in reasonable agreement with BOUT simulations with respect to the mode structure (poloidal variation of k_θ and radial localization), frequency (given a reasonable choice of E_r at the simulation boundary), and fluctuation amplitude (good agreement for $\delta n/n$ and $\delta\phi$, with reasonable correspondence for δB_θ). Parameter scans in E_r at the simulation boundary, q_{95}, and collisionality reproduce several aspects of the experimental behavior, including time variation in the QC-mode frequency and the disappearance of the QC mode as q_{95} or the edge collisionality is reduced. These observations support our identification of the QC mode in C-Mod with the resistive X-point mode observed in these BOUT simulations.

The authors acknowledge the efforts of the entire Alcator C-Mod group in carrying out the experiments reported here. In particular, we are thankful to Y. Lin and B. LaBombard for the reflectometer and the scanning probe data, respectively, and to R. H. Cohen, J. Drake, M. Greenwald, B. Rogers, T. D. Rognlien, D. D. Ryutov, and S. Wolfe for valuable discussions. This work was performed under the auspices of the U.S. Department of Energy by MIT under Contract No. DE-FC02-99ER54512, and by the University of California, Lawrence Livermore National Laboratory under Contract No. W-7405-Eng-48.

[1] W. Suttrop, Plasma Phys. Controlled Fusion **42**, Suppl. 5A, A1 (2000).
[2] H. Zohm, Plasma Phys. Controlled Fusion **38**, 105 (1996).
[3] M. Greenwald *et al.*, Phys. Plasmas **6**, 1943 (1999).
[4] R. E. Slusher *et al.*, Phys. Rev. Lett. **53**, 667 (1984).
[5] E. Marmar *et al.*, in *Proceedings of the 18th International Conference on Fusion Energy, Sorrento, 2000* http://www.iaea.org/programmes/ripc/physics/fec2000/html/node68.htm
[6] Y. Lin *et al.*, Rev. Sci. Instrum. **70**, 1078 (1999).
[7] A. E. Hubbard *et al.*, Phys. Plasmas **8**, 2033 (2001).
[8] I. H. Hutchinson *et al.*, Phys. Rev. Lett. **84**, 3330 (2000).
[9] A. Mazurenko, Ph.D. thesis, MIT Department of Physics, 2001.
[10] K. H. Burrell *et al.*, Phys. Plasmas **8**, 2153 (2001).
[11] J. A. Snipes *et al.*, Plasma Phys. Controlled Fusion **43**, L23 (2001).
[12] B. N. Rogers, J. R. Drake, and A. Zeiler, Phys. Rev. Lett. **81**, 4396 (1998).
[13] X. Q. Xu *et al.*, Phys. Plasmas **7**, 1951 (2000).
[14] J. Myra *et al.*, Phys. Plasmas **7**, 4622 (2000).
[15] L. L. Lao *et al.*, Nucl. Fusion **25**, 1611 (1985).
[16] B. N. Rogers and J. R. Drake, Phys. Plasmas **6**, 2797 (1999).
[17] I. H. Hutchinson *et al.*, Plasma Phys. Controlled Fusion **41**, A609 (1999).